DOI: 10.1002/cmdc.201300277

A Conformational Mimetic Approach for the Synthesis of Carbocyclic Nucleosides as Anti-HCV Leads

Mohan Kasula,[a] Tuniki Balaraju,[a] Massaki Toyama,[b] Anandarajan Thiyagarajan,[a] Chandralata Bal,[a] Masanori Baba,[b] and Ashoke Sharon*[a]

Computer-aided approaches coupled with medicinal chemistry were used to explore novel carbocyclic nucleosides as potential anti-hepatitis C virus (HCV) agents. Conformational analyses were carried out on 6-amino-1*H*-pyrazolo[3,4-*d*]pyrimidine (6-APP)-based carbocyclic nucleoside analogues, which were considered as nucleoside mimetics to act as HCV RNA-dependent RNA polymerase (RdRp) inhibitors. Structural insight gained from the modeling studies revealed the molecular basis behind these nucleoside mimetics. The rationally chosen 6-APP analogues were prepared and evaluated for anti-HCV activity. RdRp SiteMap analysis revealed the presence of a hydrophobic cavity near C7 of the nucleosides; introduction of bulkier substituents at this position enhanced their activity. Herein we report the identification of an iodinated compound with an EC_{50} value of 6.6 μM as a preliminary anti-HCV lead.

Introduction

Hepatitis C virus (HCV) is considered major health threat, and chronic infection can lead to liver diseases such as cirrhosis and hepatocellular carcinoma.[1] Among the number of direct-acting antiviral compounds in clinical trials or approved for use in the treatment of chronic HCV, members of the nucleoside drug class have pan-genotypic activity. The degradation of natural nucleosides to ribose may be prevented by replacing the oxygen atom of the sugar ring with a methylene group.[2]

Because of these properties, carbocyclic nucleosides have received much attention as potential chemotherapeutic agents.[3] Furthermore, the discovery of abacavir and entecavir (Figure 1) for the treatment of HIV and HBV, respectively, prompted us to explore newer carbocyclic nucleosides for the treatment of HCV. Various structural modifications have been reported in the discovery of new molecules with improved efficacy.[4] Neplanocin A (NPA, Figure 1), a carbocyclic nucleoside analogue of adenine with a cyclopentene ring in place of ribose, has broad-spectrum antiviral activity. However, its cytotoxicity precluded its development as a drug.[5] Despite several modifications in the cyclopentene ring of NPA, none of the resulting analogues showed promising activity.[6] However, base modification (7-deaza-adenine) by Chu and co-workers resulted in significant anti-HCV activity,[7] which opened the door to explore other bioisosteres of adenine. In continuation of our nucleoside mimetic design process, we recently reported that the

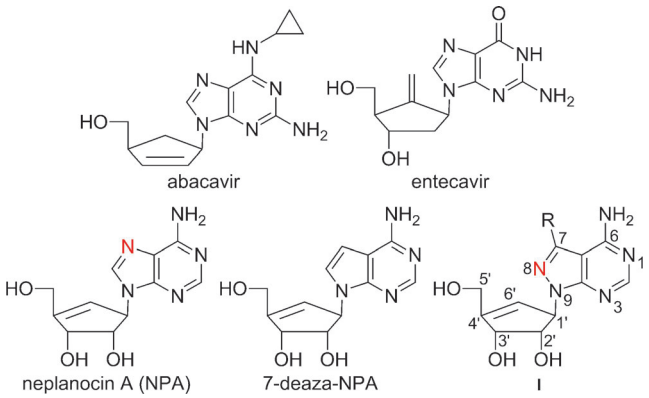

Figure 1. Structures of abacavir (approved anti-HIV drug), entecavir (approved anti-HBV drug), neplanocin A (NPA), 7-deaza-NPA, and target carbocyclic nucleosides based on 6-amino-1*H*-pyrazolo[3,4-*d*]pyrimidine (6-APP, **I**).

"*anti*" conformation of a base with a hydrogen bond donor at the 6-position and a 2′-*exo* conformation for the sugar are conducive to anti-HCV activity.[8] 1*H*-Pyrazolo[3,4-*d*]pyrimidine (PP) nucleosides shown to acquire the "*anti*" glycosyl conformation[9] have been explored extensively for a range of antiviral activities.[10] Therefore, the conformational mimetic approach was extended to select 6-amino-1*H*-pyrazolo[3,4-*d*]pyrimidine (6-APP) as a base coupled with a cyclopentene ring in order to explore a new class of carbocyclic nucleoside analogues (**I**, Figure 1) as potential anti-HCV agents.

[a] *M. Kasula, T. Balaraju, A. Thiyagarajan, Dr. C. Bal, Dr. A. Sharon*
Department of Applied Chemistry, Birla Institute of Technology
Mesra, Ranchi, Jharkhand, 835215 (India)
E-mail: asharon@bitmesra.ac.in

[b] *Dr. M. Toyama, Dr. M. Baba*
Division of Antiviral Chemotherapy, Center for Chronic Viral Disease
Kagoshima University, Sakuragaoka, Kagoshima (Japan)

Supporting information for this article is available on the WWW under http://dx.doi.org/10.1002/cmdc.201300277.

Results and Discussion

Conformational studies

We recently reported the use of a 3D model of HCV RNA-dependent RNA polymerase (HCV RdRp) complex in our nucleoside inhibitor design process and described certain conformational requirements for anti-HCV activity.[8] Previously, Marquez et al. also suggested that specific nucleoside conformations are necessary for binding with viral polymerases in order to block their function.[11] Therefore, a well-defined shape analysis is required for correlating conformation with biological activity.

The 6-APP carbocyclic nucleosides are structurally similar to NPA and 7-deaza-NPA (Figure 1). Recently, Chu and colleagues reported that 7-deaza-NPA has significant activity against HCV (2.5 μM).[7] Therefore, we analyzed the conformational behaviors of these three different compound classes (Figure 2). Among the top-five conformations of NPA (Figure 2a), four were found to be in the *syn* base disposition, whereas one showed an *anti* base disposition; all five conformers were observed to have a roughly planar sugar pucker. Both 7-deaza-NPA (Figure 2b) and the unsubstituted 6-APP carbocyclic nucleoside (Figure 2c) had four *anti* and one *syn* disposition. In addition, all the *anti* conformers of 7-deaza-NPA and the analyzed 6-APP analogue were observed in the 2′-*exo* sugar conformation. Overall, these results highlight the conformational similarity between 7-deaza-NPA and 6-APP carbocyclic nucleosides.

We also studied the conformational properties of prototype **I** analogues prior to synthesis. The conformational superposition of the 7-bromo-6-APP analogue is shown in Figure 3. Interestingly, it shows 100% *anti* base disposition with a 2′-*exo* sugar conformation. The C7-chloro and -iodo compounds had shown the same conformational behavior as the C7-bromo analogue. However, the C7-fluoro compound proved to be similar to the unsubstituted analogue. Cluster analysis of NPA (Figure 2a) suggested an 80% *syn* disposition with planar sugar puckering. These results clearly demonstrate the distinct conformational behavior of pyrazolo[3,4-*d*]pyrimidine analogues **I** relative to NPA. In our earlier studies, we found that nucleoside inhibitors may show better HCV RdRp inhibition if they have the tendency to adopt an *anti* base disposition along with a 2′-*exo* sugar conformation.[8] Therefore, we considered 6-APP carbocyclic nucleoside analogues as suitable candidates for development into a new class of anti-HCV compounds.

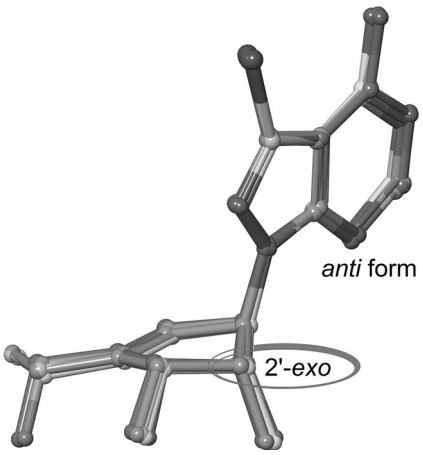

Figure 3. The top five conformational superimposition poses of 7-bromo-substituted 6-APP carbocyclic nucleoside.

Molecular docking studies

These molecules were also assessed for their ability to bind HCV RdRp. A previously reported model[12] was further refined and optimized by using a recently reported X-ray crystal structure of an HCV primer–template complex.[13] The template, primer, and metal ions were extracted from the crystal structure of the HCV RdRp complex during construction of the 3D model. The natural ATP substrate was docked into the nucleoside active site to generate the HCV RdRp–ATP model. The ATP-docked model was further subjected to 5 ns molecular dynamics (MD) simulation. The final HCV RdRp model, consisting of the template–primer complex (2:3), ATP, and two magnesium ions, was selected. The nucleoside analogues must be converted into their triphosphate form by kinase activity to act as competitive inhibitors of the natural ATP substrate. For effec-

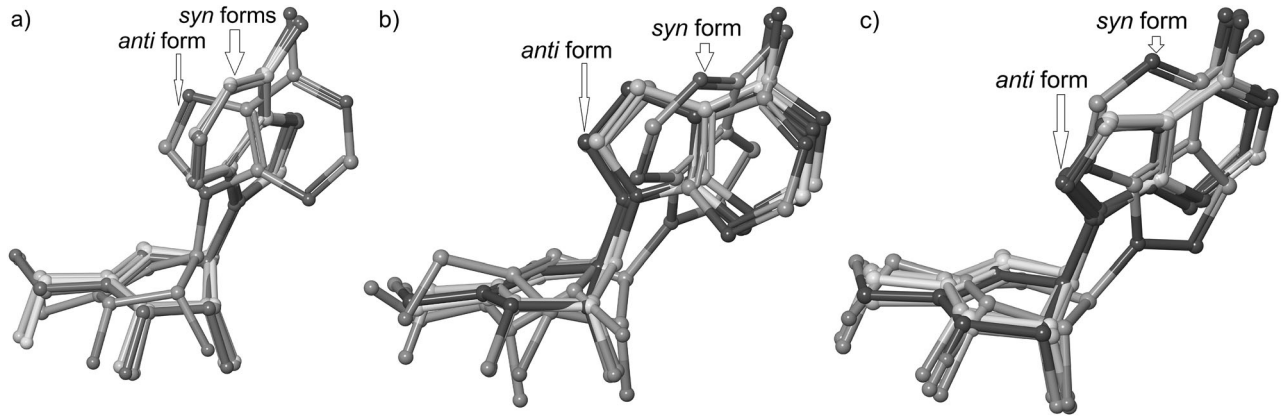

Figure 2. Top five conformers of a) NPA, b) 7-deaza-NPA, and c) 6-APP carbocyclic nucleoside (**I**, R = H) for conformational comparison.

tive comparison with ATP, the triphosphate analogues of compounds **6a**–**d** were therefore built and docked into the active site of HCV RdRp. The superimposed docking poses of **6a**–**d** triphosphates with ATP (Figure 4) suggests their ability to mimic ATP to act as HCV RdRp inhibitors.

The Glide module of Schrödinger Suite[14] was used for molecular docking to study the binding mode of compounds **6a**–**d** and to evaluate their docking scores. The Glide docking scores, conformational,[15] and drug-like properties are summarized in Table 1. Chemically and structurally, the 6-APP core, which is a single-atom-replacement bioisosteric analogue of NPA, appears to be very similar to NPA. However, the docking score (G Score) and free energy of binding (ΔG_{bind}) (Table 1) clearly indicate a difference, suggesting that the 6-APP core is more suitable as an HCV RdRp inhibitor. Moreover, substitution at C7 with bulkier groups (Cl, Br, I) provided a better energetic profile than that of the unsubstituted analogue **6a**. It also indicates the possibility of a hydrophobic cavity in the HCV RdRp active site. SiteMap analysis (Figure 5), carried out in continuation, revealed the hydrophobic nature (yellow) around the 6-APP base; however, other sub-sites were found to be charged in nature (blue, red, or pink mesh). This analysis showed a cavity available proximal to the C7 position of 6-APP in the hydrophobic region (Figure 5, yellow mesh).

The 6-APP analogues **6a**–**d** were found mostly in the *anti* conformation (Table 1, $\chi = -111$), which supports the observations from conformational studies (Figure 3). Furthermore, the degree of sugar puckering was observed to be higher ($\upsilon = 22.2$) than in NPA ($\upsilon = 15.6$). Overall, a higher level of puckering along with a 2′-*exo* conformation and *anti* base disposition can be considered as features of the best conformer to fit into the HCV RdRp active site. The QikProp module of Schrödinger was used for analyzing properties as they relate to Lipinski's rule of five[16] as well as Jorgensen's rule of three,[17] and none of the compounds violated either set of guidelines (Table 1). Furthermore, these molecules were found to be acceptable in terms of aqueous solubility and oral absorption criteria (Table 1). Thus, the preliminary computational studies provided a strong rationale to consider this new class of 6-APP-based carbocyclic nucleosides for synthesis and anti-HCV activity evaluations.

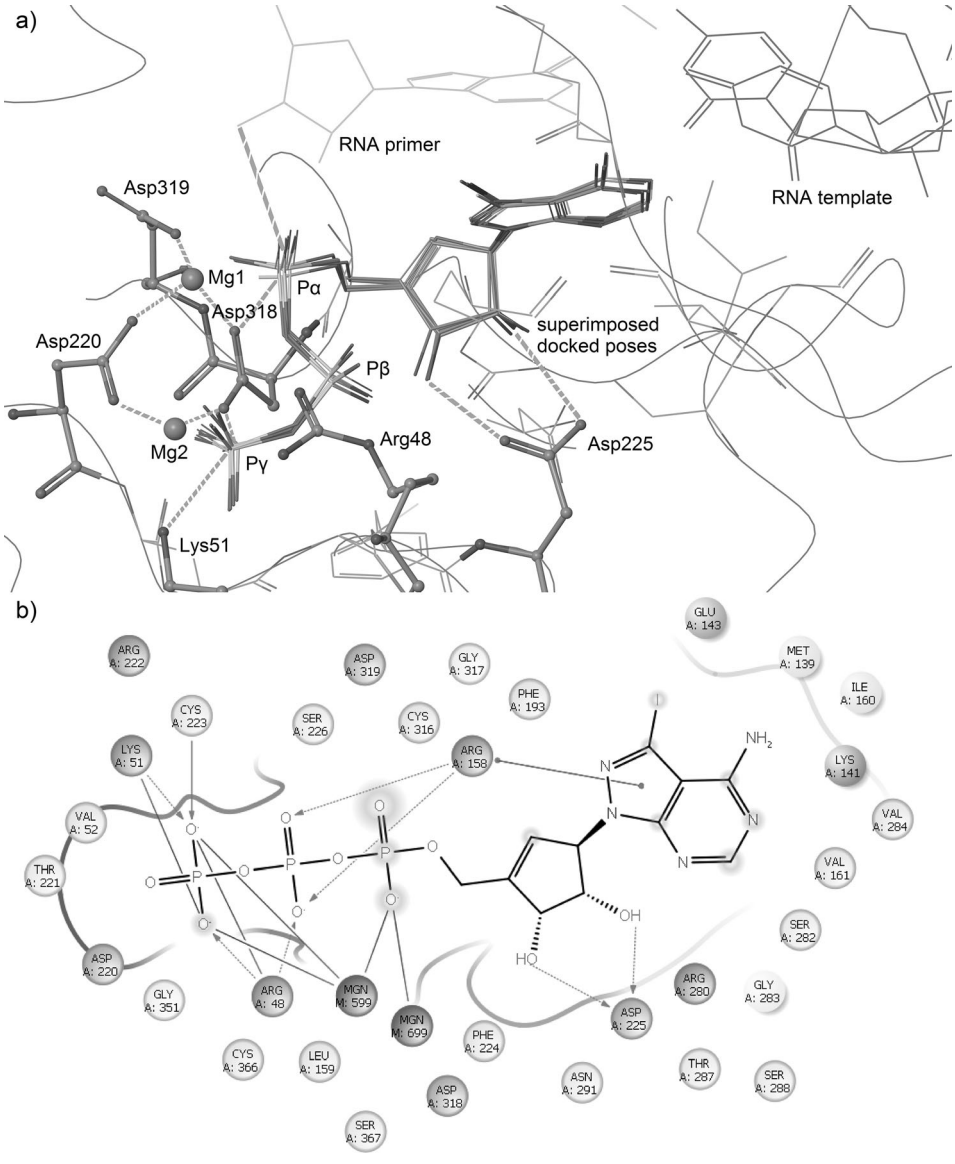

Figure 4. a) Superimposed docked poses of the triphosphate forms of **6a**–**d** and ATP in the active site of HCV-RdRp. The image shows interactions of two magnesium ions with major residues (Asp220, Asp318, and Asp319) and with the phosphates (Pα, Pβ, and Pγ) of ATP or **6a**–**d**. b) Active site binding interactions of **6d**. Metal ions (MGN) coordinate with phosphate group oxygen atoms of **6d** triphosphate; hydrogen bonds are shown as dotted arrows, and the π–cation interaction between Arg158 and the pyrazole ring is shown by the thick line flanked by filled circles.

Chemistry and anti-HCV activity

The key cyclopentene intermediate **1**, was prepared as a single isomer as per a method reported earlier[18] in eight consecutive steps by starting from commercially available D-ribose.[8] 6-APP (**2**) was synthesized by starting from malononitrile,[19] and *N-tert*-butoxycarbonyl (Boc) was used for protecting the amino group. For this purpose a solution of **2** and di-*tert*-butyl dicarbonate

Table 1. Molecular docking scores, pseudorotation analysis from conformational search, and drug-like properties of **6a–d** in comparison with NPA.

Compd	Pseudorotation Analysis[a]		Binding Score[b]		Drug Like Properties			
	Sugar Puckering	Base Disposition [%]	G Score[b]	ΔG_{bind}[c]	Human Oral Absorption [%]	QPlog S[d]	Rule Violations #5[e]	#3[f]
NPA	γ: −57, χ: −70.2, υ: 15.6, P: 344.6	*syn* (80%)	−12.5	−64.7	52.0	−1.86	0	0
6a	γ: −57, χ: −111, υ: 22.2, P: 343	*anti* (80%)	−12.8	−76.2	53.6	−1.97	0	0
6b	γ: −57, χ: −111, υ: 22.2, P: 343	*anti* (100%)	−13.1	−86.9	58.1	−2.48	0	0
6c	γ: −57, χ: −111, υ: 22.2, P: 343	*anti* (100%)	−13.2	−87.9	58.8	−2.55	0	0
6d	γ: −57, χ: −111, υ: 22.2, P: 343	*anti* (100%)	−13.2	−88.4	59.4	−2.64	0	0

[a] γ = dihedral angle to show the 5′-OH orientation, χ = dihedral angle to describe the base disposition (*syn* or *anti*) relative to the central five-membered ring, υ = planarity of central five-membered ring, P = pseudorotation phase angle to describe the overall conformation ($P = 0^\circ$ corresponds to north conformation, whereas $P = 180^\circ$ corresponds to south conformation). [b] Glide Score: the minimized poses are rescored using Schrödinger's proprietary scoring function, and the binding affinity can be estimated by G Score. [c] MM-GBSA Score: $\Delta G_{bind} = E_{complex\,(minimized)} - [E_{ligand\,(from\ minimized\ complex)} + E_{receptor}]$; ΔG_{bind} is the ligand–receptor interaction energy of the complex. [d] From −6.5 to 0.5. [e] Number of violations of Lipinski's rule of five: $M_r < 500$, QPlog $P_{octanol/water} < 5$, HBD ≤ 5, HBA ≤ 10. [f] Number of violations of Jorgensen's rule of three: QPlog $S > 5.7$, QPPCaco > 22 nm s^{-1}, primary metabolites < 7. Compounds with fewer violations of both sets of rules are more likely to be orally available.

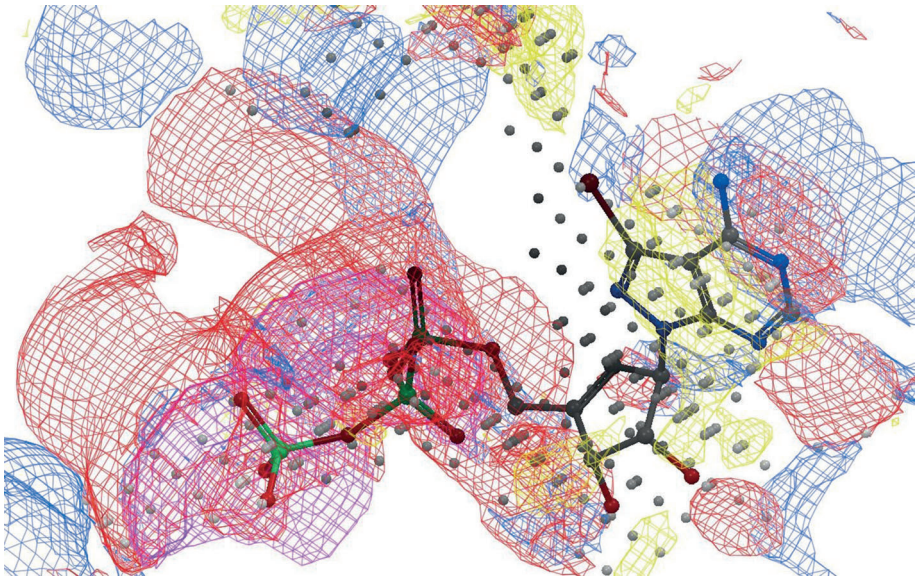

Figure 5. Various regions of the nucleoside active sites are shown in different mesh colors. Hydrophobic regions: yellow, hydrogen bond donors: blue, hydrogen bond acceptors: red, metal binding: pink.

[(Boc)$_2$O] in THF was stirred at room temperature in the presence of DMAP as catalyst (Scheme 1). Upon completion of the reaction, excess THF was removed, and the crude was dissolved in methanol and treated with saturated aqueous sodium bicarbonate at room temperature for 3 h to obtain the di-Boc derivative **3a**.

The reaction of **2** with respective *N*-halosuccinimides in DMF generated 7-halogenated derivatives **4a–c**. A similar procedure as described above was followed to furnish the di-Boc derivatives **3b–d**. Mitsunobu coupling of **3a–d** with **1** yielded **5a–d** as single products (Scheme 2). The UV spectra for compounds **5a–d** were very similar to those of their respective Boc-protected aglycons **3a–d**, indicating N9 glycosylation.[20]

In the case of N8 glycosylation, a bathochromic shift should be observed.[21] Furthermore, H-7 of **5a** was irradiated in a NOE experiment, and no correlation with any sugar ring protons was observed. Seela et al. reported earlier that irradiation of H-7 of the N8-glycosylated product showed NOEs with protons of the sugar ring.[22] Therefore, we performed a conformational search analysis of N8 and N9 isomers that could be formed during the coupling of **3a** with **1** to calculate the possible distances (Figure 6) between H-7 and cyclopentene ring protons (olefinic and protons above the plane i.e., H2′ and H3′). We found that the distances are in the NOE range for the N8 isomer, whereas they are out of NOE range for the N9 isomer (Figure 6). Finally, scrutinizing the spatial distance of the protecting groups (trityl and Boc) suggests that the N8 isomer is sterically unfavored, as the two groups may undergo steric clash. Therefore, we assigned the single products **5a–d** as N9 glycons. This regioselectivity may be attributed to the steric hindrance experienced in formation of the N8 isomer. The structural characterizations were also confirmed by NMR and COSY analysis. The 2′-H and 3′-H are in *cis*; accordingly, the NMR coupling constant was found to be 5.5 Hz.

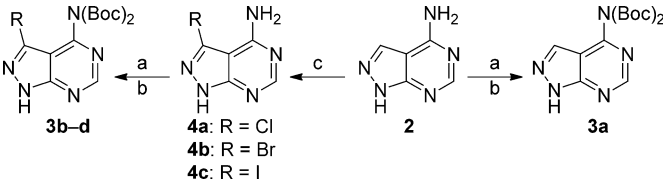

Scheme 1. Synthesis of C7-substituted and Boc-protected 6-APP bases. *Reagents and conditions*: a) (Boc)$_2$O, DMAP, THF, RT, 6 h; b) sat. NaHCO$_3$, MeOH, RT, 3 h; c) NCS/NBS/NIS, DMF, RT, 4 h.

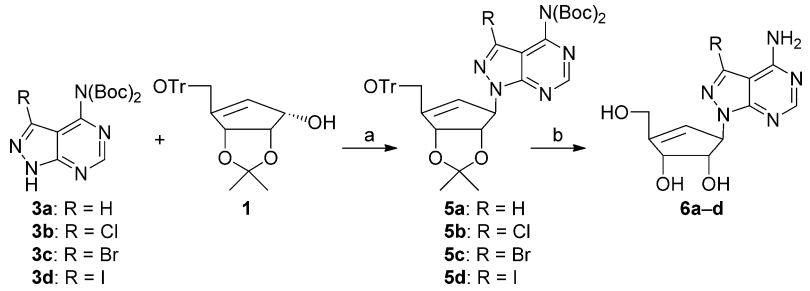

Scheme 2. Synthesis of pyrazolo[3,4-*d*]pyrimidine-based carbocyclic nucleoside analogues **6a**–**d**. *Reagents and conditions*: a) Ph_3P, DIAD, THF, 0–5 °C, 2 h; b) 10% conc. HCl in CH_3OH, 60 °C, 5 h.

The deprotection of **5a**–**d** was carried out by holding them at reflux in 10% concentrated hydrochloric acid in methanol to yield the targeted carbocyclic nucleosides **6a**–**d**. Anti-HCV assays of **6a**–**d** were carried out in the sub-genome HCV RNA replicon cells containing the luciferase gene *LucNeo#2*.[23] The anti-HCV activities of test compounds were determined from the decrease in luciferase activity. Cytotoxicity was evaluated from the decrease in viable cell numbers by using a tetrazolium dye method. EC_{50} and CC_{50} values were calculated, and the results are shown in Figure 7 and summarized in Table 2. The phenanthridinone derivative KZ-16 was used as a reference compound, which was recently reported to have selective anti-HCV activity.[23]

From the results, compounds **6a** and **6b** were found to be inactive. It was interesting to find that the introduction of bulkier halogen atoms at C7 markedly increased the activity with respect to size, along with better selectivity.

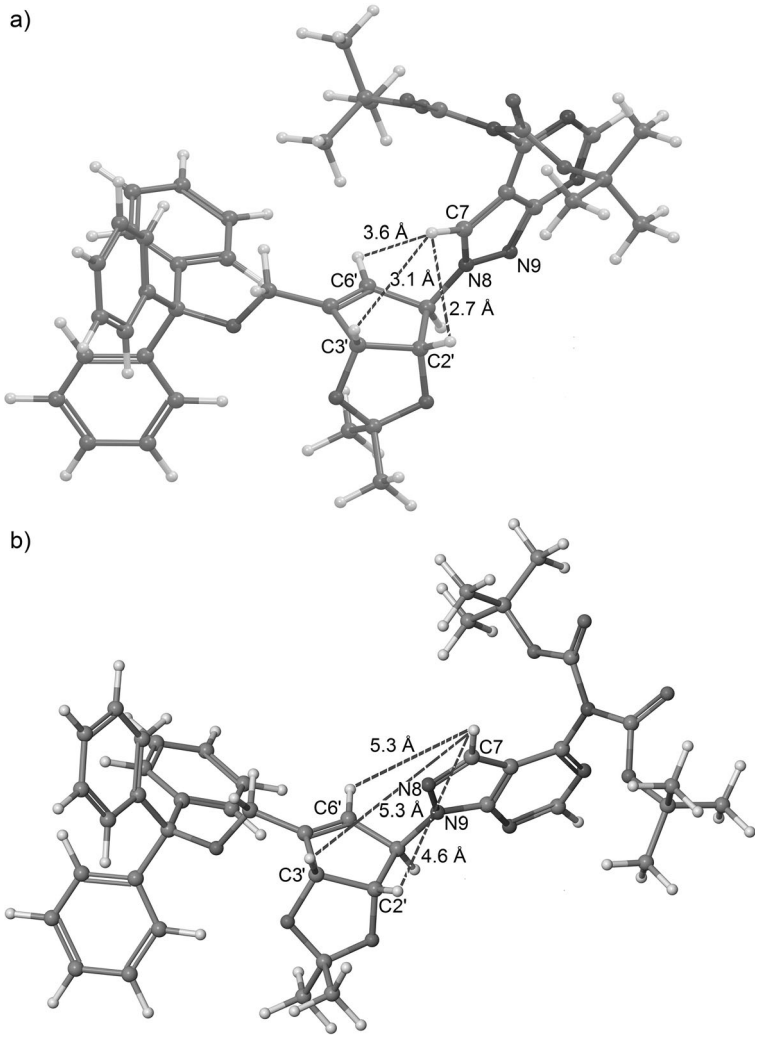

Figure 6. a) Conformational studies carried out to demonstrate intramolecular atomic distances (~3.6 Å), which illustrate the possibility for NOE in the N8 isomer only. b) The large interatomic distances (>4.6 Å) between C7–H (base) and the 2′, 3′, and 6′ CH groups of the cyclopentene ring may not give rise to NOE for the N9 isomer.

Conclusions

A conformational mimetic approach was implemented to select 6-APP carbocyclic nucleoside analogues for synthesis. The conformational search, active site analysis, and molecular docking studies provided the rationale to proceed with synthesis. The novel 6-APP-based carbocyclic nucleosides **6a**–**d** were successfully prepared, followed by anti-HCV evaluation on replicon cells. It was found that the introduction of bulky groups at C7 enhances activity. Compound **6d**, iodinated at C7, showed moderate activity (EC_{50}: 6.6 μM) with a selectivity index of 6.6, and was therefore considered a preliminary lead. However, the lack of potential activity in these compounds may be due to poor phosphorylation in replicon cells or the inability of the triphosphate forms to be recognized by RdRp. Therefore, additional experimental studies are necessary to gain knowledge into their mode of action. The results of this work set the groundwork for more detailed studies aimed at optimizing this compound class to achieve better selectivity as potential direct-acting antiviral agents.

Experimental Section

Molecular modeling

ATP was considered as a reference molecule for comparison against synthesized analogues. The triphosphate analogues of **6a**–**d** can be considered as nucleoside triphosphate mimics (NTMs) and were prepared with the builder module of Maestro followed by energy minimization (EM) through the Macromodel module. EM calculations were performed with the MMFFs force field for 5000 steps or until the energy difference between subse-

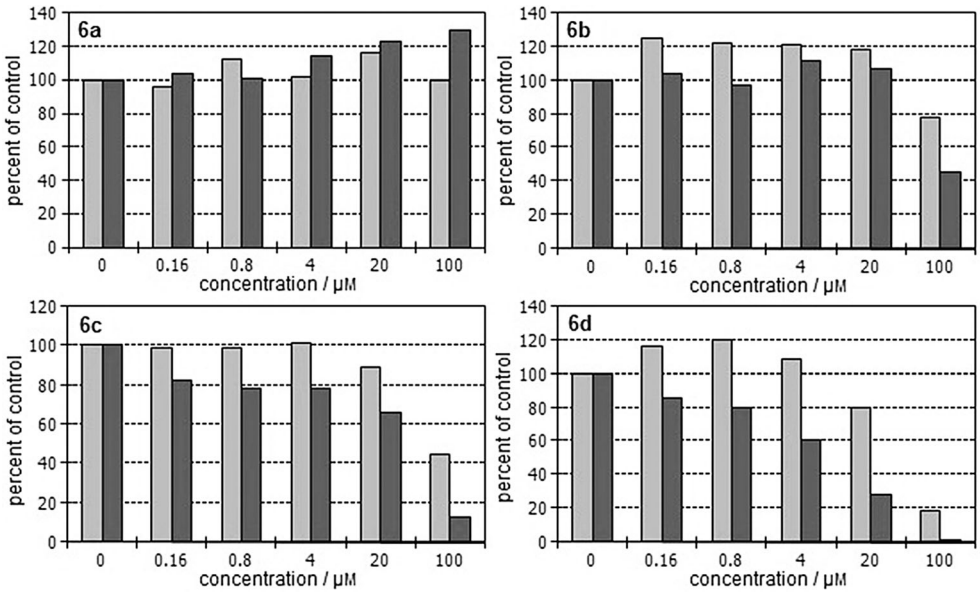

Figure 7. Anti-HCV activity of **6a–d** in replicon cells. Cell viabilities (light grey) and luciferase activities (dark grey) are shown. All experiments were carried out in duplicate, and data shown are from single representative experiments.

Table 2. Anti-HCV activity of synthesized compounds.

Compd	CC_{50} [μM][a]	EC_{50} [μM][b]	SI[c]
6a	>100	>100	–
6b	>100	87.6	–
6c	80.7	32.2	2.5
6d	43.6	6.6	6.6
KZ-16[d]	>10	0.17	58.8

[a] 50% cytotoxic concentration, determined from the decrease in viable cell counts. [b] 50% effective concentration, determined from inhibition in luciferase activity. [c] CC_{50}/EC_{50}. [d] Phenanthridinone derivative.[23]

quent structures was 0.05 kJ mol^{-1}. The initial conformations for all molecules were obtained by 5000 steps of Monte Carlo conformational search (CS) under the GB/SA continuum water solvation model using MMFFs force field and subsequent EM by the Polak–Ribiere conjugate gradient (PRCG) method. The top-five conformations were selected for conformational studies. The online server PROSIT was used to calculate geometrical parameters, including the pseudo-rotation angle of NTMs. The lowest-energy conformer of each NTM was submitted for analysis of its drug-like properties using the QikProp module of Schrödinger.

The HCV RdRp model was built as previously described[8] and refined based on the crystal structure of HCV RdRp complex (PDB ID: 4E7A).[13] ATP was docked into the nucleoside active site to generate the HCV RdRp–ATP model. The ATP-docked model was further subjected to 5 ns molecular dynamics (MD) simulation using Desmond, and the average structure was chosen. The final HCV RdRp model consists of the template–primer complex (2:3), the natural ATP substrate, along with the two Mg^{2+} ions. It was further optimized and checked by the Protein Preparation module and EM by Macromodel using the OPLS2005 force field for 5000 steps with the GB/SA continuum water solvation model. The lowest-energy conformer of triphosphate analogues of **6a–d** (NTMs) were selected for molecular docking studies. The nature of active site (hydrophobic, hydrophilic, metal binding, etc.) was analyzed by SiteMap analysis, using the default method of the SiteMap module of Schrödinger. A receptor grid was generated around ATP (the natural nucleoside triphosphate) by using the Glide receptor grid generation utility. Molecular docking studies were conducted with NTMs as ligand at the predefined receptor grid using the extra precision (XP) mode of Glide to investigate the top-five poses and binding score. The top-docked poses were evaluated using Prime with MMGBSA free energy of binding (ΔG_{bind}) to estimate the NTM–HCV RdRp interaction energy (Table 1). The MMGBSA scoring calculates the difference between the energy of the NTM-bound complex and the sum of the energies of unbound HCV RdRp: $E_{binding} = [E_{complex} - (E_{HCV\text{-}RdRp} + E_{NTM})]$.

Chemistry

All reactions were carried out in oven-dried glassware under nitrogen atmosphere. The chemicals and solvents were purchased from Spectrochem, Across, Rankem, or Sigma–Aldrich. D-Ribose was purchased from Carbosynth Limited. Melting points were recorded on a Veego melting point apparatus. Analytical thin-layer chromatography (TLC) was performed on pre-coated plates (silica gel 60 F_{254}) purchased from Merck. Purification by gravity column chromatography was carried out on silica gel (100–200 mesh). An Elico UV/Vis spectrophotometer was used for recording UV spectra. Optical rotations of optically active compounds were measured on a Rudolph Autopol I instrument. ^{1}H and ^{13}C NMR spectra were obtained on Varian or Bruker spectrometers (400 and 100 MHz) using $CDCl_3$ or [D_6]DMSO as solvents. Peaks are recorded with the following abbreviations: s, singlet; bs, broad singlet; d, doublet; t, triplet; q, quartet; m, multiplet; *J*, coupling constant (Hz).

General procedure for the synthesis of 6a–d

DIAD (3.75 mmol) was added dropwise to a mixture of the appropriate compound **3a–d** (1.5 mmol), key cyclopentene intermediate **1** (1.57 mmol), and Ph_3P (3.75 mmol) in THF at 0 °C. The reaction mixture was brought to RT, and stirring continued. Reaction completion was analyzed by TLC, the solvent was evaporated under reduced pressure, and the crude was purified by column chromatography on silica gel by eluting with up to 30% EtOAc in hexane to give coupling products **5a–d** in 70–80% yields.

The deprotection of trityl, acetonide, and Boc groups of **5a–d** was carried out by heating at 60 °C in 10% HCl in MeOH. After completion (monitored by TLC), the reaction mixture was concentrated under reduced pressure, and the solid was washed with acetone to yield pure HCl salts of carbocyclic nucleosides **6a–d** in 70–85% yield.

Di-Boc-protected 1-((4*R*)-2,2-dimethyl-6-((trityloxy)methyl)-4,6a-dihydro-3a*H*-cyclopenta[*d*][1,3]dioxol-4-yl)-1*H*-pyrazolo[3,4-*d*]pyrimidin-4-amine (5a): Yield: 80%; mp: 81 °C; HRMS (*m/z*): 768.7283 [M^++Na]; UV (MeOH): λ_{max}=265.7 nm; ^{1}H NMR (400 MHz, $CDCl_3$): δ=8.76 (s, 1H, 2-CH), 8.13 (s, 1H, 7-CH), 7.20–7.45 (m, 15H, trityl), 6.05–6.10 (m, 2H, 1′,6′-CH), 5.33–5.35 (d, J=5.5 Hz, 1H, 2′-CH), 4.87–4.88 (d, J=5.5 Hz, 1H, 3′-CH), 3.95–3.98 (d, J=14.8 Hz, 1H, 5′-CH_2), 3.78–3.82 (d, J=14.8 Hz, 1H, 5′-CH_2), 1.55 (s, 18H, Boc-6CH_3), 1.45 (s, 3H, CH_3), 1.33 ppm (s, 3H, CH_3).

Di-Boc-protected 3-chloro-1-((4*R*)-2,2-dimethyl-6-((trityloxy)-methyl)-4,6a-dihydro-3a*H*-cyclopenta[*d*][1,3]dioxol-4-yl)-1*H*-pyrazolo[3,4-*d*]pyrimidin-4-amine (5b): Yield: 83%; mp: 70–74 °C; MS (ESI) (*m/z*): [M^+−100 (Boc)] 680.0, [M^++2−100] 682.0; UV (MeOH): λ_{max}=263.0 nm; ^{1}H NMR (400 MHz, $CDCl_3$): δ=8.96 (s, 1H, 2-CH), 7.47–7.22 (m, 15H, trityl), 6.05–6.09 (m, 2H, 1′,6′-CH), 5.33–5.34 (d, J=5.7 Hz, 1H, 2′-CH), 4.87–4.88 (d, J=5.7 Hz, 1H, 3′-CH), 3.96–4.00 (d, J=15.4 Hz, 1H, 5′-CH_2), 3.81–3.84 (d, J=15.4 Hz, 1H, 5′-CH_2), 1.49 (s, 3H, CH_3), 1.47 (s, 18H, Boc-6CH_3), 1.44 ppm (s, 3H, CH_3).

Di-Boc-protected 3-bromo-1-((4*R*)-2,2-dimethyl-6-((trityloxy)-methyl)-4,6a-dihydro-3a*H*-cyclopenta[*d*][1,3]dioxol-4-yl)-1*H*-pyrazolo[3,4-*d*]pyrimidin-4-amine (5c): Yield: 82%; mp: 85–87 °C; MS (*m/z*): [M^+−100] 724.0, [M^++2−100] 726.0; UV (MeOH): λ_{max}= 263 nm; ^{1}H NMR (400 MHz, $CDCl_3$): δ=8.96 (s, 1H, 2-CH), 7.21–7.46 (m, 15H, trityl) 6.04–6.08 (m, 2H, 1′,6′-CH), 5.32–5.34 (d, J=5.8 Hz, 1H, 2′-CH), 4.87–4.88 (d, J=5.9 Hz, 1H, 3′-CH), 3.95–3.99 (d, J= 15.3 Hz, 1H, 5′-CH_2), 3.80–3.83 (d, J=15.3 Hz, 1H, 5′-CH_2), 1.44 (s, 18H, Boc-6CH_3), 1.42 (s, 3H, CH_3), 1.33 ppm (s, 3H, CH_3).

Di-Boc-protected 3-iodo-1-((4*R*)-2,2-dimethyl-6-((trityloxy)methyl)-4,6a-dihydro-3a*H*-cyclopenta[*d*][1,3]dioxol-4-yl)-1*H*-pyrazolo-[3,4-*d*]pyrimidin-4-amine (5d): Yield: 85%; mp: 89–99 °C; MS (ESI) (*m/z*): [M^++1] 872.0; UV (MeOH): λ_{max}=264 nm; ^{1}H NMR (400 MHz, $CDCl_3$): δ=8.97 (s, 1H, 2-CH), 7.21–7.46 (m, 15H, trityl), 6.04–6.08 (m, 2H, 1′,6′-CH), 5.33–5.35 (d, J=5.8 Hz, 1H, 2′-CH), 4.88–4.90 (d, J=5.9 Hz, 1H, 3′-CH), 3.95–3.99 (d, J=15.3 Hz, 1H, 5′-CH_2), 3.80–3.84 (d, J=15.3 Hz, 1H, 5′-CH_2), 1.45 (s, 3H, CH_3), 1.42 (s, 18H, Boc-6CH_3), 1.33 ppm (s, 3H, CH_3).

(1*S*,2*R*,5*R*)-5-(4-Amino-1*H*-pyrazolo[3,4-*d*]pyrimidin-1-yl)-3-(hydroxymethyl)cyclopent-3-ene-1,2-diol (6a): Yield: 60%; mp: 189–192 °C; HRMS (*m/z*): 286.1638 [M^++Na]; $[\alpha]_D^{21}$= −120.29 $cm^3 g^{-1} dm^{-1}$ (c=0.38 MeOH); UV (MeOH): λ_{max}=264 nm; ^{1}H NMR (400 MHz, [D_6]DMSO): δ=9.71 (bs, 1H, NH_2), 8.83 (bs, 1H, NH_2), 8.45 (s, 2H, 2-CH & 7-CH), 5.66–5.67 (m, 1H, 1′-CH), 5.56–5.57 (m, 1H, 6′-CH), 4.41–4.42 (m, 1H, 2′-CH), 4.29–4.32 (m, 1H, 3′-CH), 4.06–4.15 (m, 2H, 5′-CH_2), 3.16–3.65 ppm (bs, 3H, 2′, 3′ & 5′-OH); ^{13}C NMR (100 MHz, [D_6]DMSO): δ=153.09, 151.55, 150.50, 148.57, 135.31, 123.86, 100.01, 76.86, 72.53, 67.15, 58.92 ppm.

(1*S*,2*R*,5*R*)-5-(4-Amino-3-chloro-1*H*-pyrazolo[3,4-*d*]pyrimidin-1-yl)-3-(hydroxymethyl)cyclopent-3-ene-1,2-diol (6b): Yield: 71%; mp: 206–208 °C; MS (ESI) (*m/z*): [M^+] 297.8, [M^++2] 299.8; UV (MeOH): λ_{max}=267 nm; $[\alpha]_D^{21}$= −164.04 $cm^3 g^{-1} dm^{-1}$ (c=0.15 MeOH); ^{1}H NMR (400 MHz, [D_6]DMSO): δ=9.40 (bs, 1H, NH_2), 8.73 (bs, 1H, NH_2), 8.50 (s, 1H, 2-CH), 5.84–6.21 (bs, 3H, 2′, 3′ & 5′-OH), 5.66–5.67 (m, 1H, 1′-CH), 5.57–5.58 (m, 1H, 6′-CH), 4.38–4.40 (m, 1H, 2′-CH), 4.24–4.27 (m, 1H, 3′-CH), 4.06–4.15 ppm (m, 2H, 5′-CH_2); ^{1}H NMR (400 MHz, [D_6]DMSO, D_2O exchange): δ=8.29 (s, 1H, 2-CH), 5.62–5.65 (m, 2H, 1′ & 6′-CH), 4.40–4.41 (m, 1H, 2′-CH), 4.20–4.23 (m, 1H, 3′-CH), 4.08–4.10 ppm (m, 2H, 5′-CH_2); ^{13}C NMR (100 MHz, [D_6]DMSO): δ=152.76, 152.71, 151.13, 150.00, 133.38, 123.34, 97.55, 76.89, 72.42, 67.58, 58.93 ppm.

(1*S*,2*R*,5*R*)-5-(4-Amino-3-bromo-1*H*-pyrazolo[3,4-*d*]pyrimidin-1-yl)-3-(hydroxymethyl)cyclopent-3-ene-1,2-diol (6c): Yield: 80%; mp: 189–190 °C; MS (ESI) (*m/z*): [M^+] 342.0, [M^++2] 344.0; UV (MeOH): λ_{max}=262 nm; $[\alpha]_D^{21}$= −155.62 $cm^3 g^{-1} dm^{-1}$ (c=0.18 MeOH); ^{1}H NMR (400 MHz, [D_6]DMSO): δ=9.18–9.25 (bs, 1H, NH_2), 8.47 (s, 1H, 2-CH), 8.18–8.28 (bs, 1H, NH_2), 5.66–5.67 (m, 1H, 1′-CH), 5.56–5.57 (m, 1H, 6′-CH), 4.45–5.22 (bs, 3H, 2′, 3′ & 5′-OH), 4.37–4.39 (m, 1H, 2′-CH), 4.24–4.27 (m, 1H, 3′-CH), 4.06–4.14 ppm (m, 2H, 5′-CH_2); ^{13}C NMR (100 MHz, [D_6]DMSO): δ=153.48, 153.02, 150.97, 150.54, 123.53, 120.16, 99.77, 76.92, 72.39, 67.57, 58.93 ppm.

(1*S*,2*R*,5*R*)-5-(4-Amino-3-iodo-1*H*-pyrazolo[3,4-*d*]pyrimidin-1-yl)-3-(hydroxymethyl)cyclopent-3-ene-1,2-diol (6d): Yield: 81%; mp: 194–196 °C; MS (ESI) (*m/z*): [M^++1] 390.0; $[\alpha]_D^{21}$= −147.88 $cm^3 g^{-1} dm^{-1}$ (c=0.24 MeOH); UV (MeOH): λ_{max}=264 nm; ^{1}H NMR (400 MHz, [D_6]DMSO): δ=9.18–9.22 (bs, 1H, NH_2), 8.49 (s, 1H, 2-CH), 8.02–8.21 (bs, 1H, NH_2), 5.64–5.65 (m, 1H, 1′-CH), 5.56–5.57 (m, 1H, 6′-CH), 4.61–5.22 (bs, 3H, 2′, 3′ & 5′-OH), 4.38–4.39 (m, 1H, 2′-CH), 4.26–4.29 (m, 1H, 3′-CH), 4.07–4.11 ppm (m, 2H, 5′-CH_2); ^{13}C NMR (100 MHz, [D_6]DMSO): δ=153.06, 152.10, 150.23, 148.93, 123.23, 102.68, 92.39, 76.45, 71.82, 67.00, 58.39 ppm.

Anti-HCV activity

The anti-HCV activities of test compounds **6a–d** were determined in *LucNeo#2*[24] cells by using the previously described method with some modifications.[25] All compounds were dissolved in DMSO at 20 mM or higher to exclude the cytotoxicity of DMSO and stored at −20 °C until use. Huh-7 cells containing self-replicating sub-genomic replicons with a luciferase reporter, *LucNeo#2*, were grown and cultured in Dulbecco's modified Eagle's medium (DMEM) with high glucose (Gibco/BRL) supplemented with 10% heat-inactivated fetal bovine serum (Gibco/BRL), 100 U mL^{-1} penicillin G, and 100 μg mL^{-1} streptomycin. *LucNeo#2* cells were maintained in DMEM containing 1 mg mL^{-1} G418 (Nakarai Tesque). Briefly, cells (5×10^3 cells per well) were cultured in a 96-well plate in the absence of G418 and in the presence of various concentrations of test compounds. After incubation at 37 °C for 3 days, the culture medium was removed, and cells were washed twice with phosphate-buffered saline. Lysis buffer was added to each well, and the lysate was transferred to the corresponding well of a non-transparent 96-well plate. Luciferase activity was measured after the addition of luciferase reagent in a luciferase assay system kit (Promega), using a luminometer with automatic injectors (Berthold Technologies). The number of viable cells was determined by a dye-based method using the water-soluble tetrazolium Tetracolor One (Seikagaku Corporation), according to the manufacturer's instructions.

Acknowledgements

We acknowledge financial support from the Department of Science & Technology, Delhi (India) through grant no. SR/FT/CS-001/2009. M.K. and T.B. thank CSIR (India) for the award of a Senior Research Fellowship (SRF). A.S. thanks the Department of Biotechnology, India for modeling software support. The authors acknowledge Dr. Reddy's Institute of Life Sciences, Hyderabad for use of the NMR–Mass Spectrometry Facility, and the Central Instrument Facility at BIT Mesra for analytical support.

Keywords: antiviral agents · carbocyclic nucleosides · hepatitis C · inhibitors · RNA-dependent RNA polymerase

[1] D. Lavanchy, *Clin. Microbiol. Infect.* **2011**, *17*, 107 – 115.
[2] M. T. Crimmins, *Tetrahedron* **1998**, *54*, 9229 – 9272.
[3] a) X. F. Zhu, *Nucleosides Nucleotides Nucleic Acids* **2000**, *19*, 651 – 690; b) M. Ferrero, V. Gotor, *Chem. Rev.* **2000**, *100*, 4319 – 4348.
[4] a) A. B. Eldrup, M. Prhavc, J. Brooks, B. Bhat, T. P. Prakash, Q. Song, S. Bera, N. Bhat, P. Dande, P. D. Cook, *J. Med. Chem.* **2004**, *47*, 5284 – 5297; b) A. Cho, O. L. Saunders, T. Butler, L. Zhang, J. Xu, J. E. Vela, J. Y. Feng, A. S. Ray, C. U. Kim, *Bioorg. Med. Chem. Lett.* **2012**, *22*, 2705 – 2707.
[5] G. Wolfson, J. Chisholm, A. H. Tashjian, S. Fish, R. H. Abeles, *J. Biol. Chem.* **1986**, *261*, 4492 – 4498.
[6] a) X. Liao, G. Butora, D. B. Olsen, S. S. Carroll, D. R. McMasters, J. F. Leone, M. Stahlhut, G. A. Doss, L. Yang, M. MacCoss, *Tetrahedron Lett.* **2008**, *49*, 4149 – 4152; b) H. R. Lee, J. A. Kang, A. Y. Park, W. H. Kim, P. Chun, J. Kim, J. A. Kim, B. Lee, L. S. Jeong, H. R. Moon, *Bull. Korean Chem. Soc.* **2009**, *30*, 2043 – 2050; c) H. Zhang, R. F. Schinazi, C. K. Chu, *Bioorg. Med. Chem.* **2006**, *14*, 8314 – 8322; d) N. Hamon, J. P. Uttaro, C. Mathe, C. Perigaud, *Bioorg. Chem.* **2010**, *38*, 275 – 278.
[7] H. J. Kim, A. Sharon, C. Bal, J. Wang, M. Allu, Z. Huang, M. G. Murray, L. Bassit, R. F. Schinazi, B. Korba, C. K. Chu, *J. Med. Chem.* **2009**, *52*, 206 – 213.
[8] A. Thiyagarajan, M. T. A. Salim, T. Balaraju, C. Bal, M. Baba, A. Sharon, *Bioorg. Med. Chem. Lett.* **2012**, *22*, 7742 – 7747.
[9] S. Sprang, R. Scheller, D. Rohrer, M. Sundaralingam, *J. Am. Chem. Soc.* **1978**, *100*, 2867 – 2872.
[10] a) Y. V. Dobrynin, T. Bektemirov, T. Ivanova, E. Chekunova, O. Andzhaparidze, I. Korbukh, Y. B. Bulychev, N. Yakunina, M. Preobrazhenskaya, *Pharm. Chem. J.* **1980**, *14*, 279 – 284; b) D. Smee, P. McKernan, L. D. Nord, R. Willis, C. Petrie, T. Riley, G. Revankar, R. Robins, R. Smith, *Antimicrob. Agents Chemother.* **1987**, *31*, 1535 – 1541; c) L. M. Beauchamp, J. V. Tuttle, M. E. Rodriguez, M. L. Sznaidman, *J. Med. Chem.* **1996**, *39*, 949 – 956; d) A. E. Rashad, A. H. Shamroukh, R. E. Abdel-Megeid, A. Mostafa, M. A. Ali, K. Banert, *Nucleosides Nucleotides Nucleic Acids* **2010**, *29*, 809 – 820.
[11] V. E. Marquez, T. Ben-Kasus, J. J. Barchi, Jr., K. M. Green, M. C. Nicklaus, R. Agbaria, *J. Am. Chem. Soc.* **2004**, *126*, 543 – 549.
[12] T. Balaraju, C. Bal, A. Sharon, *Antiviral Res.* **2012**, A14.
[13] R. T. Mosley, T. E. Edwards, E. Murakami, A. M. Lam, R. L. Grice, J. Du, M. J. Sofia, P. A. Furman, M. J. Otto, *J. Virol.* **2012**, *86*, 6503 – 6511.
[14] Schrödinger LLC, New York, NY (USA), **2011**.
[15] G. Sun, J. H. Voigt, I. V. Filippov, V. E. Marquez, M. C. Nicklaus, *J. Chem. Inf. Comput. Sci.* **2004**, *44*, 1752 – 1762.
[16] C. A. Lipinski, F. Lombardo, B. W. Dominy, P. J. Feeney, *Adv. Drug Delivery Rev.* **2001**, *46*, 3 – 26.
[17] W. L. Jorgensen, E. M. Duffy, *Adv. Drug Delivery Rev.* **2002**, *54*, 355 – 366.
[18] J. H. Cho, D. L. Bernard, R. W. Sidwell, E. R. Kern, C. K. Chu, *J. Med. Chem.* **2006**, *49*, 1140 – 1148.
[19] R. K. Robins, *J. Am. Chem. Soc.* **1956**, *78*, 784 – 790.
[20] J. D. Anderson, N. K. Dalley, G. R. Revankar, R. K. Robins, *J. Heterocycl. Chem.* **1986**, *23*, 1869 – 1878.
[21] a) H. B. Cottarn, G. R. Revankar, R. K. Robins, *Nucleic Acids Res.* **1983**, *11*, 871 – 882; b) F. W. Lichtenthaler, E. Cuny, *Chem. Ber.* **1981**, *114*, 1610 – 1623.
[22] F. Seela, A. M. Jawalekar, L. Sun, P. Leonard, *Nucleosides Nucleotides Nucleic Acids* **2005**, *24*, 1485 – 1505.
[23] M. T. Salim, H. Aoyama, K. Sugita, K. Watashi, T. Wakita, T. Hamasaki, M. Okamoto, Y. Urata, Y. Hashimoto, M. Baba, *Biochem. Biophys. Res. Commun.* **2011**, *415*, 714 – 719.
[24] K. Goto, K. Watashi, T. Murata, T. Hishiki, M. Hijikata, K. Shimotohno, *Biochem. Biophys. Res. Commun.* **2006**, *343*, 879 – 884.
[25] M. P. Windisch, M. Frese, A. Kaul, M. Trippler, V. Lohmann, R. Bartenschlager, *J. Virol.* **2005**, *79*, 13778 – 13793.

Received: June 19, 2013
Published online on ■■ ■■, 0000

A well-defined shape analysis is needed for correlating conformation with biological activity. Our nucleoside mimetic design process involves conformational cluster analysis to evaluate the preferred "*anti*" conformation of the base with respect to the 6-position hydrogen bond donor and 2′-*exo* conformations for anti-HCV activity. In neplanocin A, the adenine base shows 80% *syn* with only 20% in the preferred *anti* conformation in carbocyclic nucleosides.

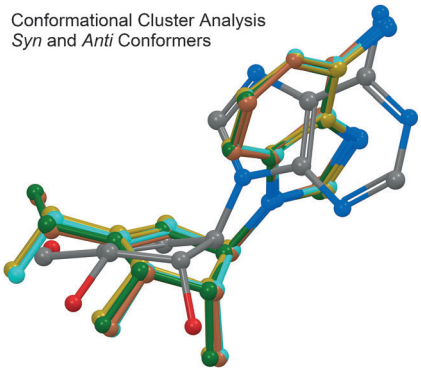

*M. Kasula, T. Balaraju, M. Toyama, A. Thiyagarajan, C. Bal, M. Baba, A. Sharon**

■■ – ■■

A Conformational Mimetic Approach for the Synthesis of Carbocyclic Nucleosides as Anti-HCV Leads